# Nonlinear Optical Pulse Suppression via Ultrafast Photoinduced Electron Transfer in an Aggregated Perylene Diimide/Oligothiophene Molecular Triad

**ARTICLE** *in* THE JOURNAL OF PHYSICAL CHEMISTRY A · DECEMBER 2013

Impact Factor: 2.69 · DOI: 10.1021/jp409065b · Source: PubMed



**7 AUTHORS**, INCLUDING:

Matthew Sartin
RIKEN
**16** PUBLICATIONS **247** CITATIONS
SEE PROFILE

Stephen Barlow
Georgia Institute of Technology
**284** PUBLICATIONS **11,480** CITATIONS
SEE PROFILE

Seth Marder
Georgia Institute of Technology
**667** PUBLICATIONS **26,664** CITATIONS
SEE PROFILE

Joseph W. Perry
Georgia Institute of Technology
**321** PUBLICATIONS **12,109** CITATIONS
SEE PROFILE

THE JOURNAL OF PHYSICAL CHEMISTRY A

Article

pubs.acs.org/JPCA

# Nonlinear Optical Pulse Suppression via Ultrafast Photoinduced Electron Transfer in an Aggregated Perylene Diimide/Oligothiophene Molecular Triad

Matthew M. Sartin,[†,⊥] Chun Huang,[‡,⊥] Ariel S. Marshall, Nikolay Makarov,[§] Stephen Barlow, Seth R. Marder,* and Joseph W. Perry*

School of Chemistry and Biochemistry and Center for Organic Photonics and Electronics, Georgia Institute of Technology, Atlanta, Georgia 30332-0400, United States

Supporting Information

**ABSTRACT:** A donor−acceptor−donor triad material in which two quinquethiophene moieties are attached via nonconjugated, flexible bridges to the 1,7-positions (80% isomer) and 1,6-positions (20% isomer) of a perylene diimide (**PDI-5T**) has been synthesized, and its nonlinear suppression of nanosecond laser pulses in the 680−750 nm range has been studied. The kinetics of the photoinduced charge separation processes have been characterized using femtosecond transient pump−probe spectroscopy. Excitation of either the quinquethiophene donor or perylene diimide acceptor leads to ultrafast (<700 fs) photoinduced charge separation, yielding quinquethiophene and perylene diimide radical ions that are strongly absorbing in the red−near-IR region. Despite the short lifetime (52 ps) of the charge-separated state, reasonably strong nonlinear suppression of nanosecond pulses, with figures-of-merit up to 14, has been realized with 4 mM solutions of **PDI-5T**. Although the radical ion absorption (RIA) is much stronger at 750 nm than that at 680 or 700 nm, the best optical suppression figures-of-merit were observed at 680 and 700 nm. Comparison of the optical parameters at these wavelengths suggests that the stronger ground-state absorption, due to aggregates of **PDI-5T**, is responsible for the enhanced figure-of-merit at the shorter wavelength.

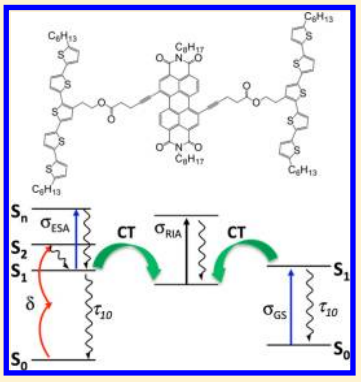


## INTRODUCTION

Passive nonlinear optical materials with high ambient transmission that can strongly attenuate intense laser pulses are becoming increasingly important for the protection of optical sensors.[1] Strong laser pulse suppression has been achieved with materials exhibiting nonlinear absorption (NLA) mechanisms that rely on the spectral overlap of the photon wavelengths for excitation by one-photon (1PA) or two-photon (2PA) absorption from the ground state with that of a more strongly absorbing, photogenerated transient state. One effective method for achieving this is the use of multichromophoric systems consisting of covalently linked electron donors and electron acceptors, such that photoexcitation of either moiety results in the generation of an absorbing radical ion pair.[2−4] The donor and acceptor can be chosen independently, such that molecules with radical ions possessing large molar absorptivities or 2PA cross sections in the spectral region of interest can be attached to donors or acceptors with weaker ground-state absorptivity in the same region. The ability to further tune the NLA wavelength or bandwidth via structural modifications and the possibility of preparing polymers of the donor and acceptor moieties have led to further development in this area.[5]

In previous work, we demonstrated nonlinear optical pulse suppression with a bis(dialkylaminostyryl)carbazole/perylene diimide (PDI) dyad[4] via excitation into the 2PA absorption band of the donor moiety at wavelengths where the PDI radical anion exhibited strong absorption. In addition, we observed a substantial contribution to the concentration of radical ions resulting from excitation into the linear absorption tail of aggregates formed in the highly concentrated solutions of these dyads. Although the dyad with the greater aggregate absorption exhibited the best optical pulse suppression (see Table S1, Supporting Information), the overall benefit of utilizing the aggregate absorption in NLA materials based on photogenerated charge carrier absorption is not completely clear. In such systems, the advantage of the greater number of radical ions generated via 1PA pumping is countered by the reduced transmittance of ambient light at the wavelength of excitation.

Additionally, many aggregated molecular systems show a reduction in the lifetime of the photogenerated charge-separated state relative to that of nonaggregated systems, as a result of the shorter donor−acceptor distance. For example, one of the dyads in the previous study[4] exhibited a 13 ns decay of its charge-separated state in dilute solution but showed enhanced recombination rates at the high concentrations for which strong aggregate absorption was observed. Pulse suppression using transient states that are much shorter lived

**Received:** September 10, 2013
**Revised:** December 10, 2013
**Published:** December 16, 2013

  

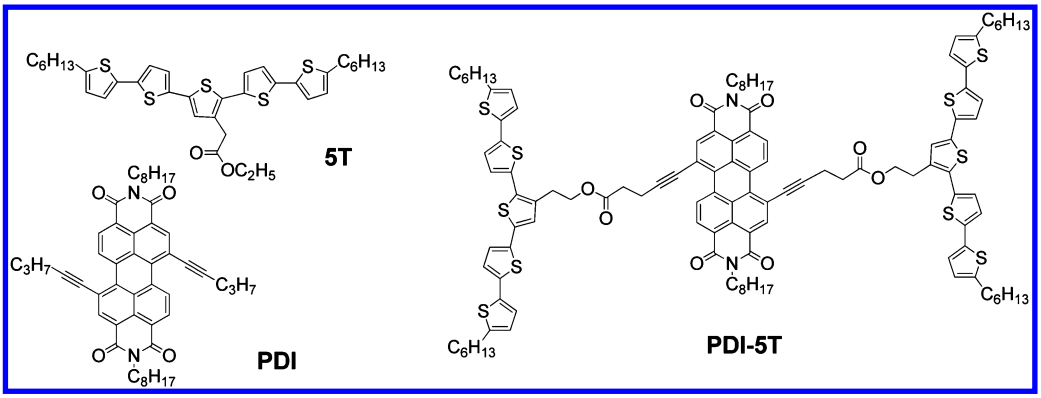


**Figure 1.** The chemical structures of **PDI-5T** triad and model compounds (only 1,7-isomers shown for **PDI** and **PDI-5T**).

than the excitation pulse width typically leads to lower transient state populations, which are less beneficial for protecting optical sensors.[6] It is, therefore, important to consider the effects of aggregation when examining optical pulse suppression performance.

Here, we report on the photoinduced charge transfer (CT) and nonlinear optical pulse suppression properties of a donor−acceptor−donor triad compound, wherein quinquethiophene (5T) donors that are attached to the 1,7(1,6) "bay" positions of a PDI acceptor moiety (**PDI-5T**, Figure 1; only the 1,7 substituted isomer is illustrated). The charge-transport properties of bay-substituted PDIs and oligothiophenes have been studied previously,[7] and *N*-substituted PDIs have been examined for photoinduced charge separation (CS) in the context of photovoltaic applications;[8−11] however, to the best of our knowledge, studies on the optical pulse suppression by such materials have not been reported. **PDI-5T** was designed such that, upon 1PA or 2PA excitation, a radical ion pair could be generated, in which both the radical cation[12] and radical anion[13] exhibit strong absorption at the excitation wavelength. We aim to better understand the role of 1PA by intramolecular and intermolecular aggregates on the nonlinear optical pulse suppression in solutions of flexible, linked donor−acceptor−donor chromophores. We first characterize the electrochemistry and linear optical properties of the **PDI-5T** triad and the corresponding model compounds, as well as the aggregate absorption. Next, we investigate the transient absorption (TA) spectra and kinetics of the **PDI-5T** triad and the model compounds at various concentrations. Lastly, we examine the nonlinear optical suppression of nanosecond pulses by **PDI-5T** and its aggregates in the band-edge region between 680 and 750 nm. As we will show, the overlap of the RIA band with that of the 1PA or 2PA absorption band of the triad and the 1PA of the aggregates gives rise to effective optical pulse suppression.

## EXPERIMENTAL SECTION

**General.** Most organic and inorganic chemicals were obtained from Aldrich and Alfa Aesar. Palladium-based catalysts were purchased from Strem Chemicals and used without further purification. The $^{1}$H and $^{13}$C NMR spectra were collected on a Bruker 400 or 500 MHz spectrometer using tetramethylsilane (TMS; $\delta$ = 0 ppm) as an internal standard. Mass spectra were measured on a VG Instruments 70-SE using the electron impact (EI) mode or on an Applied Biosystems 4700 Proteomics Analyzer using MALDI mode. Atlantic Microlabs performed elemental analyses by using a LECO 932 CHNS elemental analyzer. Solution UV−vis absorption spectra were recorded on a UV3101PC (Shimadzu) spectrophotometer, and emission spectra were recorded using a Spex Fluorolog-2. Electrochemical measurements were carried out under nitrogen in deoxygenated 0.1 M solutions of tetra-*n*-butylammonium hexafluorophosphate in dry dichloromethane, using a computer-controlled BAS 100B electrochemical analyzer, a glassy carbon working electrode, a platinum wire auxiliary electrode, and a Ag wire anodized with AgCl as a pseudoreference electrode. Cyclic voltammograms are presented in Figure S1 (Supporting Information). Potentials were referenced to the ferrocenium/ferrocene ($FeCp_2^{+/0}$) couple by using ferrocene or decamethylferrocene ($FeCp^*_2$) as an internal standard (Table 1).

**Table 1. Electrochemical Half-Wave Potentials[a] of PDI-5T and Model Compounds**

| materials | oxidation | reduction |
|---|---|---|
| **PDI-5T** | +0.34 (2), 0.67 (2) | −1.06 (1), −1.20 (1) |
| **PDI** | | −1.05 (1), −1.22 (1) |
| **5T** | +0.39 (1), 0.61 (1) | |

[a]Potentials (V) versus $FeCp_2^{+/0}$ in $CH_2Cl_2$ (0.1 M [$^n$Bu$_4$N][PF$_6$]), obtained using a 50 mV s$^{-1}$ scan rate for each material; relative currents associated with each peak are given in parentheses.

**Femtosecond TA Measurements.** The excitation pulses for femtosecond TA experiments were generated using an optical parametric amplifier (TOPAS, Spectra-Physics) pumped by the 800 nm output of a Ti:Sapphire regenerative amplifier (Spitfire, Spectra-Physics), operating at a repetition rate of 1 kHz. The TOPAS output is tunable in the range of 290−2900 nm. The pump beam was attenuated to 1 $\mu$J/pulse using an ND filter. Approximately 5% of the 800 nm Spitfire output was used to generate the white light continuum probe in the visible (420−950 nm) and NIR (800−1600 nm) in crystalline plates supplied with the commercially available Helios spectrometer (Ultrafast Systems, Sarasota, FL), which was used to collect the data. The pump was chopped at 500 Hz to alternate pump and probe pulses. At each temporal delay, the signal was averaged for 2 s. The time resolution for this system is ∼200 fs in the visible and ∼300 fs in the NIR.

**Nanosecond Optical Pulse Suppression Measurements.** The excitation source for nanosecond NLA measurements was the output of an optical parametric amplifier (Quanta-Ray MOPO 730) pumped by the third harmonic of a Q-switched Nd:YAG laser (Quanta-Ray PRO 250). A fraction of the OPA output was redirected by a beam splitter placed


dx.doi.org/10.1021/jp409065b | J. Phys. Chem. A 2014, 118, 110−121

**Scheme 1. Synthetic Scheme for PDI-5T**[a]

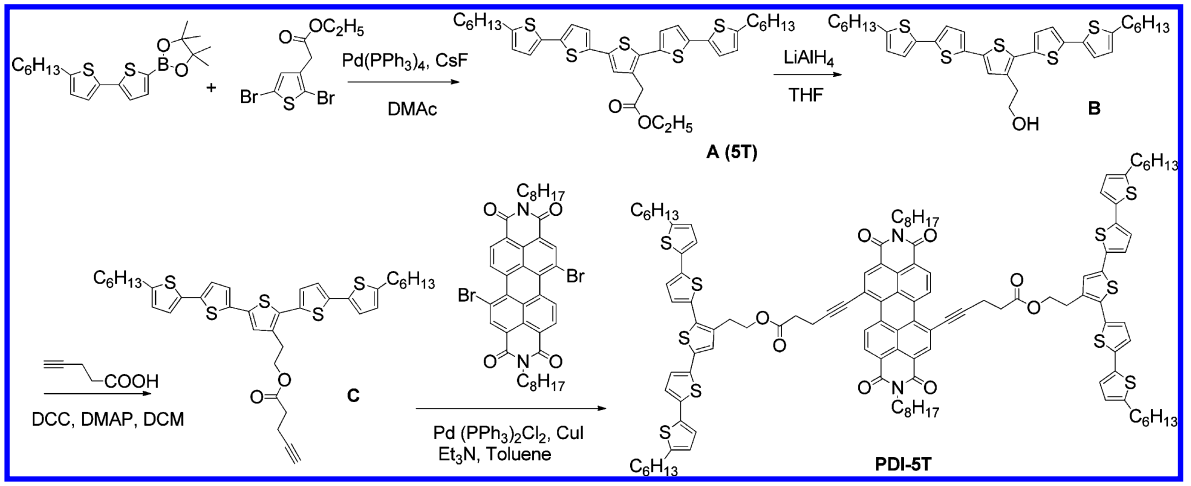


[a]Only the 1,7-isomer is shown.

before the sample to serve as a reference for the pulse energy. The remainder of the output was focused in an f/5 geometry into a 2 mm sample cell. The position of the focus in the cell was established by translating a solution of a nonlinear absorber along the laser beam and placing the cell at the position of minimum transmittance. The size of the focal spot was determined by scanning a 5 $\mu$m pinhole across the focus of the beam and measuring the transmitted power as a function of position. A typical fwhm of the resulting plot of 14 $\mu$m was taken to be the beam diameter at the focus. Both the transmitted signal and reference were detected by photoreceivers (New Focus), whose output was averaged using a boxcar averager (Stanford Research Systems).

## RESULTS AND DISCUSSION

**Synthesis.** Scheme 1 shows the synthesis of the **PDI-5T** triad. The ester-functionalized 5T, compound **A** (**5T**), was synthesized via a Suzuki coupling reaction between 5′-hexyl-2,2′-bithiophene-5-boronic acid pinacol ester and ethyl-2,5-dibromothiophene-3-acetate,[14,15] using $Pd(PPh_3)_4$ as a catalyst. To avoid hydrolysis of the ester group, a water- and base-free Suzuki coupling reaction with cesium fluoride as a cocatalyst was used, with anhydrous dimethylacetamide as the solvent, to prepare the desired product.[16] The ester group in compound **A** was then converted into an alcohol functionality using $LiAlH_4$ as a reducing agent to give compound **B** in quantitative yield. Compound **B** was then reacted with pent-4-ynoic acid in the presence of a mixture of dicyclohexylcarbodiimide (DCC) and *p*-dimethylaminopyridine (DMAP) to afford a 5T linked to a terminal alkyne, compound **C**, in a yield of ∼71%. The triad **PDI-5T** was then prepared through a Sonogashira cross-coupling reaction[17] between compound **C** and a mixture of *N*,*N*′-dioctyl-1,7-dibromo-3,4,9,10-PDI and *N*,*N*′-dioctyl-1,6-dibromo-3,4,9,10-PDI,[18] with $Pd(PPh_3)_4$ as a catalyst in a procedure similar to that used for other 1,(6)7-dialkynyl PDIs.[13] The model compound, **PDI**, was prepared following a modification of the procedure described in the literature.[13,19] Because the starting dibromo PDI derivative is a mixture of two isomers, the **PDI** model and **PDI-5T** are also a mixture of two isomers. The isomers were not readily separated by purification methods such as column chromatography[20] or crystallization.[21] The $^1$H NMR spectrum of **PDI** indicates a ∼4:1 ratio of 1,7- and 1,6-isomers. The isomers of **PDI-5T** were not readily distinguishable by $^1$H NMR spectroscopy but were prepared from the same batch of dibromo PDI starting material as **PDI** and therefore are likely to be present in the same isomer ratio. All data discussed in the rest of this paper refer to the as-synthesized isomer mixtures.

**Electrochemistry.** The electrochemical properties of the triad and model compounds were investigated using cyclic voltammetry (CV) in anhydrous dichloromethane, and the results are shown in Table 1 and Figure S1 (Supporting Information). The half-wave reduction potential values ($E_{1/2}{}^{0/1-}$ and $E_{1/2}{}^{1-/2-}$, defined as $(E_{pa} + E_{pc})/2$, where $E_{pa}$ and $E_{pc}$ are peak oxidation and reduction potentials, respectively) of both **PDI-5T** and **PDI** are around −1.1 V for the first reduction and ∼−1.2 V for the second reduction versus $FeCp_2{}^{+/0}$. The first and second oxidation processes for **5T** were observed at +0.39 V and ∼+0.61 V, respectively, versus $FeCp_2{}^{+/0}$; **PDI-5T** shows similar features, each corresponding to the first and second oxidation of *both* 5T moieties within the triad. These observations, together with the UV−vis absorption spectra of **PDI-5T** discussed above, suggest limited ground-state electronic coupling between chromophores within the triad. According to these electrochemical data and the optical data given below, electron transfer from either the excited 5T moiety to the PDI moiety or excited PDI to 5T should be highly exergonic (driving force of ∼1.1 and 0.7 eV, respectively, even when neglecting Coulombic stabilization in the resultant ion pair). This observation is consistent with the strong fluorescence quenching for **PDI-5T** in solution following either donor or acceptor excitation (see below).

**1PA Absorption Spectroscopy.** 1PA absorption spectra of **PDI-5T** and model compounds in toluene are presented in Figure 2. The **5T** chromophore exhibits a single, broad peak with a 1PA absorption maximum wavelength ($\lambda_{max}$) at 410 nm, similar to that observed for unsubstituted 5T ($\lambda_{max}$ = 417 nm in dioxane).[22] **PDI** exhibits a highly structured absorption, with maxima at 478, 511, and 550 nm. These bands are ∼20 nm red-shifted from those of PDIs without bay substitution,[23,24] consistent with what is seen for other bay-alkynylated PDIs, where the conjugation of the PDI moiety can be extended onto the acetylene substituents.[13,25]

The absorption spectrum of **PDI-5T** shows clearly identifiable PDI and 5T contributions. However, when compared with the sum of the absorption spectra of the **PDI**


dx.doi.org/10.1021/jp409065b | J. Phys. Chem. A 2014, 118, 110−121

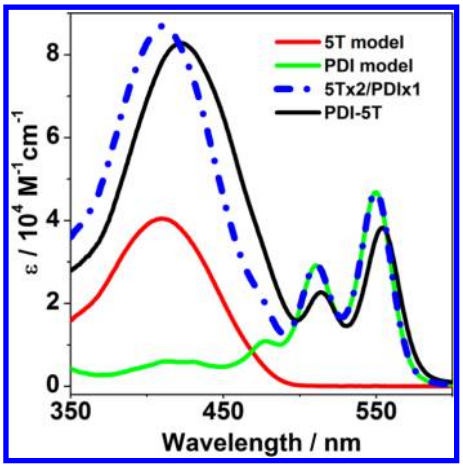


**Figure 2.** Molar absorptivity of dilute samples in toluene: 61 $\mu$M **PDI-5T**, 130 $\mu$M **5T**, 113 $\mu$M **PDI**, and the sum of the molar absorptivities of 2 **5Ts** to 1 **PDI**.

and **5T** compounds, after scaling the molar extinction coefficient of **5T** by a factor of 2, the triad spectrum shows slightly red-shifted bands (3−6 nm) with lower peak extinction coefficients. In addition to the small shifts, the spectrum of **PDI-5T** shows an absorption tail extending to ∼700 nm (Figure 3) that is not observed in the absorption spectra of the model compounds. This tail is tentatively assigned to an intramolecular CT complex absorption between the 5T and PDI moieties, the formation of which is facilitated by the flexibility of the linker groups. Indeed, the tail extends over a similar wavelength range as the low-energy absorptions observed for PDIs bay-substituted with directly linked oligothiophenes, where, however, the low-energy absorptions are much stronger due to stronger donor−acceptor coupling.[8]

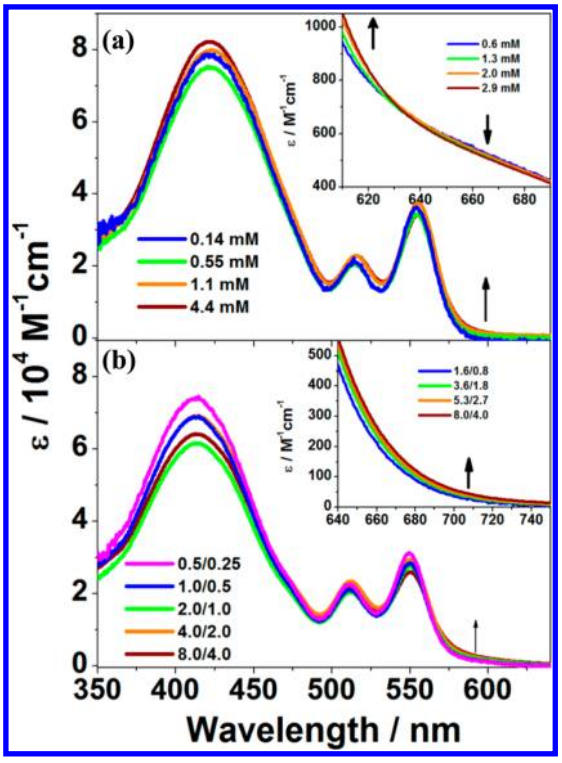


**Figure 3.** (a) Molar absorptivity of highly concentrated toluene solutions of **PDI-5T** in a 50 $\mu$m cell. (Inset) Triad absorption tail in a 2 mm cell. (b) 2:1 **5T**/**PDI** co-dissolved in toluene (concentrations in mM given as **5T**/**PDI** in the legend) in a 50 $\mu$m cell. (Inset) **5T**/**PDI** solution in a 2 mm cell. Molar absorptivities were estimated based on the **PDI** concentration.

At the high concentrations used for NLA studies, both **PDI-5T** and a solution containing both model compounds, co-dissolved in a 2:1 5T-to-PDI ratio, exhibit small changes in their absorption spectra at long wavelengths. PDI−PDI aggregation is typically suggested by a decrease in the ratio of the (0,1) to (0,0) absorption bands and usually accompanied by red shifting and broadening of those bands.[26,27] As shown in Figure 3a, **PDI-5T** exhibits neither of these effects, but it does show a small increase of the extinction coefficient in the tail of the absorption spectrum at wavelengths to the blue of 620 nm, suggesting that an intermolecular complex between 5T and PDI units forms in concentrated solutions. This effect also occurs in the concentrated solutions of the co-dissolved model compounds (Figure 3b), where an increase in the long-wavelength tail near 640 nm is observed and is assigned to **5T** and **PDI** aggregation. Some possible PDI−PDI aggregation is suggested by the slight change in intensity ratio of the PDI absorption bands.

The UV−vis−NIR absorption spectra of the radical cations of **5T** and radical anions of **PDI** are presented in Figure 4. The

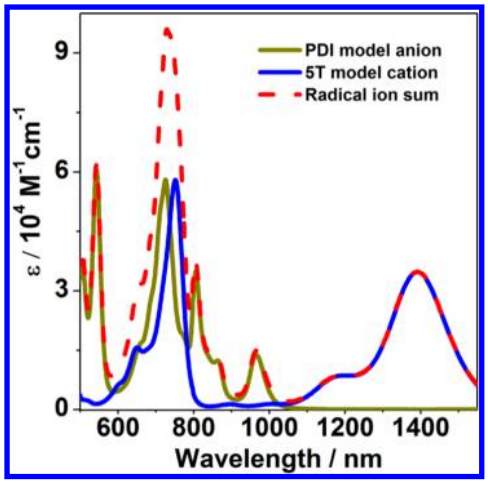


**Figure 4.** Molar absorptivity of radical ions of **5T** in $CH_2Cl_2$ and **PDI** in THF, along with the sum of the absorptivities overlaid.

spectrum of the **PDI** radical anion exhibits two sharp bands at 724 and 805 nm in THF, both of which are somewhat red-shifted from the bands seen for radical anions of PDI compounds without bay substitution,[4,28] as well as two weaker absorption bands at lower energy. The absorption spectrum of the **5T** radical cation in $CH_2Cl_2$ is typical of an oligothiophene radical cation, with strong bands peaking at 752 and 1380 nm. These values are somewhat red-shifted from those seen for the unsubstituted 5T radical cation itself in the same solvent (720, 1265 nm),[29] likely due to the effects of the terminal alkyl groups and the substituent on the central thiophene unit. Addition of the two radical ion spectra produces a maximum molar absorptivity ($\varepsilon_{max}$) of 94 000 $M^{-1}$ $cm^{-1}$ at 740 nm.

**Fluorescence Spectroscopy.** Fluorescence spectra of **PDI-5T** and the model compounds are presented in Figure 5. The **5T** chromophore was excited at 420 nm, yielding a broad, vibronically structured emission spectrum with well-defined maxima at 494, 528, and 567 nm and shoulders at ∼625


dx.doi.org/10.1021/jp409065b | J. Phys. Chem. A 2014, 118, 110−121

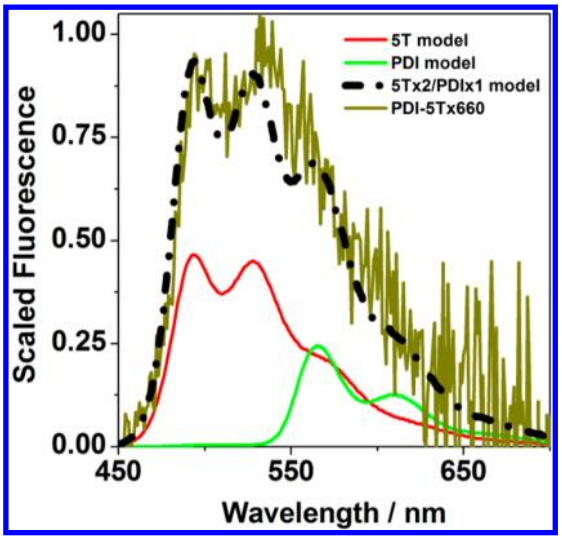


**Figure 5.** Fluorescence spectra of dilute samples dissolved in toluene, scaled based on their ground-state absorption. The sum of the fluorescence of a solution with a 2:1 ratio of **5T** and **PDI** is included for comparison with **PDI-5T** fluorescence scaled by a factor of 660.

and 688 nm, similar to that observed for other oligothiophenes.[22,30] The fluorescence quantum yield of **5T** is 0.23, similar to that for unsubstituted 5T in benzene (0.34).[22] In that report, most of the singlet deactivation was assigned to intersystem crossing to a nonemissive triplet state. Excitation of **PDI** at 550 nm gives a structured emission spectrum, with maxima at 575, 610, and 662 nm and a quantum yield of 0.80. This quantum yield is slightly smaller than that observed for a PDI without bay substituents[24] due to the electronic effects of the bay substituents.

**PDI-5T** shows extremely weak fluorescence compared with the model compounds. Upon excitation of the donor moiety at 420 nm, an emission spectrum resembling a combination of the **5T** and **PDI** emission spectra is observed with a total quantum yield of $\sim 6 \times 10^{-4}$. This weak emission suggests that there is efficient CT quenching of the excited donor moiety. The presence of a rather small emission contribution from the **PDI** might result from energy transfer from the excited donor moiety or direct excitation of the acceptor moiety absorption at the same wavelength.

**2PA Absorption.** 2PA spectra of **PDI** and **5T** are shown in Figure S2 (Supporting Information). 2PA spectra of molecular variants of both the donor[31] and acceptor[32] moieties in **PDI-5T** have been reported previously. Between 650 and 1000 nm, the 2PA spectrum of **PDI** is similar to that observed for a PDI derivative without bay substituents in the previous study.[32] **PDI** exhibits a peak 2PA cross section of 470 GM at 669 nm and 2PA cross sections ranging from 15 GM at 750 nm to 230 GM at 700 nm and 280 GM at 680 nm, the latter wavelengths of which correspond to those for optical pulse suppression measurements discussed later. **5T** exhibits a peak 2PA cross section of ~60 GM at 714 nm and 2PA cross sections ranging from ~35 GM at 750 and 680 nm to 55 GM at 700 nm. These relatively small 2PA cross sections are expected to make minor contributions to the NLA at high intensity. The emission of **PDI-5T** was too weak to obtain a reliable 2PA spectrum and cross section values with the 2PA-induced fluoresence method.

**Time-Resolved Spectroscopy.** To identify the positions of the ESA bands and the associated time constants of the model compounds, we performed TA measurements on **5T** and **PDI**. The transient spectra are presented in Figure 6a, and the time constants for the $S_1$ decay are given in Table 2. At

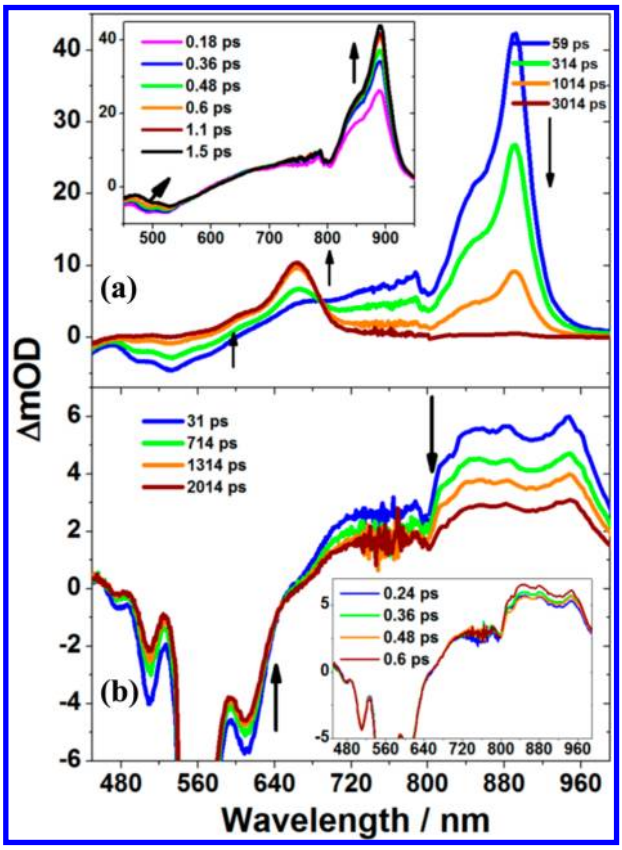


**Figure 6.** TA spectra of (a) 58 $\mu$M **5T** in toluene excited at 430 nm (OD = 0.4) and (b) 52 $\mu$M **PDI** in toluene, excited at 550 nm (OD = 0.49). The insets present the early time spectra, and the ordinates are in ΔmOD.

early times, we observe negative optical density change (ΔOD) signals, with minima at 518 and 489 nm. The first 1.5 ps of spectral evolution are characterized by the simultaneous decay and red shift of the negative ΔOD, with a time constant of ~300 fs, during which the 518 and 489 nm peaks shift to 528 and 494 nm, respectively, which we assign to stimulated

**Table 2. Time Constants for Growth and Decay Processes for Model Compounds, Triads, and Co-Dissolved Model Compounds**

| | | | process and $\tau$ (ps) | |
|---|---|---|---|---|
| materials | concentration | $\lambda_{exc}$ (nm) | initial decay | $S_1$ decay |
| **5T** | 58 $\mu$M | 430 | 0.4 ± 0.1[a] | 730 ± 10[c] |
| **PDI** | 52 $\mu$M | 550 | n/a CS[a,b] | 5500 ± 300[c] CR[a,b,d] |
| **PDI-5T** | 29 $\mu$M | 430 | 0.7 ± 0.1 | 56 ± 3, 210 ± 50 |
| | | 550 | 0.5 ± 0.1 | 57 ± 3, 350 ± 80 |
| **PDI-5T** | 4 mM | 650 | <0.5 | 52 ± 5 |
| **PDI/5T** | 4 mM:8 mM | 650 | <0.5 | 90 ± 10, 1900 ± 200 |

[a]Time constants ($\tau$) determined by TA. [b]CS = charge separation; CR = Charge recombination. [c]$S_1$ lifetime measured by TCSPC for model compounds only. [d]As discussed in the text, all but the concentrated **PDI-5T** sample shows nonexponential decays, and the data were fit to biexponential functions.


dx.doi.org/10.1021/jp409065b | J. Phys. Chem. A 2014, 118, 110−121

emission (SE). The slight red shift of the SE peaks in time suggests a decrease in the $S_0-S_1$ energy gap following excitation, which could result from planarization of the oligomer[22] or solvent or vibronic relaxation. Coincident with this process, a strong ESA band at 889 nm grows in with a rise time of ~400 fs, consistent with planarization of the chain. Both the 889 nm band and the SE decay with a time constant of ~600 ps, supporting the assignment to $S_1$ (Figure S3a, Supporting Information). The decay of these bands coincides with the growth of a new band at 662 nm; a similar, long-lived transient band observed in other oligothiophenes has previously been assigned to triplet−triplet absorption.[22,33] TCSPC measurements indicate a fluorescence decay time of 730 ps (Figure S4, Supporting Information), in reasonable agreement with the SE decay time. Our results are comparable to previously reported, time-resolved studies of unsubstituted 5T's[34−36] that show TA bands at ~630 and ~820 nm, corresponding to triplet and singlet excited states, respectively.

The TA spectra of **PDI** in toluene excited at 550 nm are shown in Figure 6b. The spectra are relatively constant in shape, over time, and consist primarily of a broad absorption in the region between 800 and 980 nm. The rise time of the **PDI** signal is instrument response function (IRF)-limited, as shown in Figure S3b (Supporting Information). The TA shows a very slow decay; the lifetime of the lowest singlet excited state was estimated by TCSPC to be 5.5 ns, consistent with other PDI-based materials.[37]

In order to assess the extent of CS in **PDI-5T** in toluene solution, we performed TA spectroscopy with excitation primarily of **5T** at 430 nm, as presented in Figure 7a. The band at 889 nm is assigned to ESA from the 5T donor moiety, based on its similarity to the $S_n \leftarrow S_1$ feature observed in TA spectra of **5T**, although its position partially overlaps that of the RIA bands observed at later time delays. Similarly, the absorption band at 712 nm has contributions assignable both to the 5T and PDI moiety radical ions, as well as the PDI moiety ESA. The absorption band centered at 1395 nm corresponds to the peak in the linear absorption spectrum of the **5T** radical cation. In the spectral regions containing both RIA and ESA, the large number of exponential functions required to describe the kinetics resulted in large uncertainty in the time constants. On the other hand, the 1395 nm 5T moiety radical cation band contains no overlapping absorption from excited-state processes; therefore, the rise and decay of the absorption at this wavelength was used to obtain the time constants for CS and charge recombination (CR) through exponential fits. The kinetic traces are presented in Figure S5a (Supporting Information). For excitation of **PDI-5T** at 430 nm, the CS time constant obtained with this method is 700 fs. The long-lived triplet absorption observed in the **5T** ESA spectrum is not observed in **PDI-5T**, likely due to its slow formation rate relative to the CS rate. The CR in **PDI-5T** is also a fairly fast process (Figure 7a, inset). The decay of the radical cation TA band was fit to a double-exponential function, which resulted in time constants of $\tau_1$ = 56 ps and $\tau_2$ = 210 ps (Figure S5a, Supporting Information). **PDI-5T** also has a flexible chain connecting the donor and acceptor; therefore, the donor−acceptor distance is also likely to be variable in this case, and we used a double-exponential fit to characterize the major time constants.

Excitation of the **PDI** moiety of **PDI-5T** in toluene at 550 nm yields essentially complete CS, as shown in the transient spectra shown in Figure 7b. The 889 nm band that was

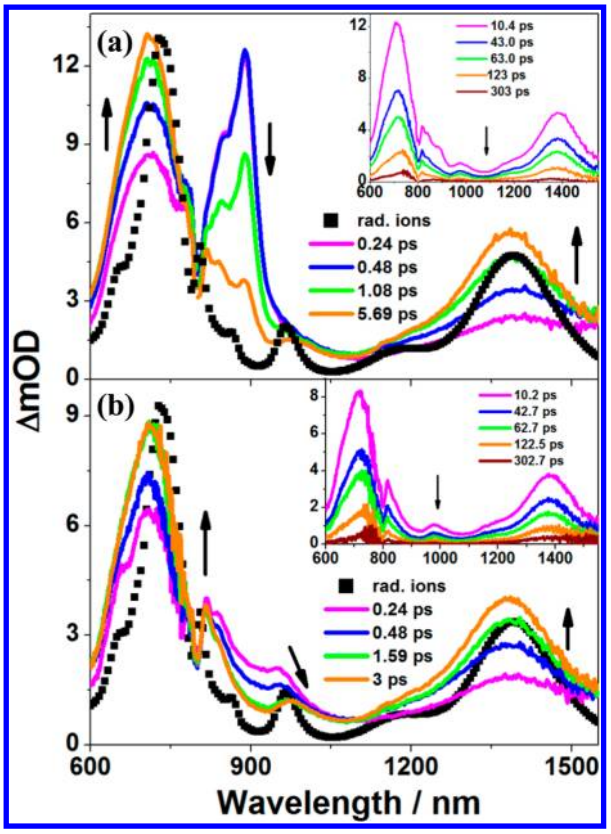


**Figure 7.** TA spectra of (a) 29 $\mu$M **PDI-5T** in toluene, excited at 430 nm (OD = 0.46). (b) TA spectra of 29 $\mu$M **PDI-5T** in toluene, excited at 550 nm (OD = 0.21). The insets present the long-time dynamics, and the ordinates are in ΔmOD. Black squares overlaid on the transient spectra represent a scaled sum of the radical anion and cation absorption spectra.

assigned to the $S_n \leftarrow S_1$ transition of the **5T** moiety in the case of 430 nm excitation is not observed as the excitation is below the **5T** band edge. The **5T** radical cation absorption at 1360 nm grows with a rise time of ~500 fs. The peak appearing at 965 nm is characteristic of the PDI radical anion spectrum, although overlapping ESA bands precluded accurate determination of the rise time of this peak. After ~3 ps, the spectrum resembles that of the sum of the radical ion spectra, indicating essentially complete CS. The CS rates obtained by excitation of the 5T or PDI moiety in **PDI-5T** are similar to one another. Slower CS has been observed previously under donor excitation than for that for acceptor excitation in related oligothiophene−PDI materials, and this has been attributed to energy transfer to the PDI moiety preceding CS.[9,10] However, with the very rapid CS observed in **PDI-5T**, it is not clear whether energy transfer precedes or competes with CS. The faster CS rate upon PDI excitation in **PDI-5T** may be a consequence of having two 5T donor groups available for CS. The existence of a weak CT band in the linear absorption spectrum of these molecules suggests that there may be sufficient electronic coupling between the donor and acceptor, as well as the driving force for CS, that energy transfer is not necessary.

**Dynamics of PDI-5T and Model Compound Solutions at High Concentration.** TA measurements of **PDI-5T** at high concentrations (~4 mM in toluene) were performed to understand the transient behavior of these materials under the conditions used for the NLA experiments described below. With excitation at 650 nm into the 1PA spectral tail of **PDI-5T**,


dx.doi.org/10.1021/jp409065b | J. Phys. Chem. A 2014, 118, 110−121

excitation of both the inter- and intramolecular aggregate CT absorption is possible. As shown in Figure 8a, the characteristic

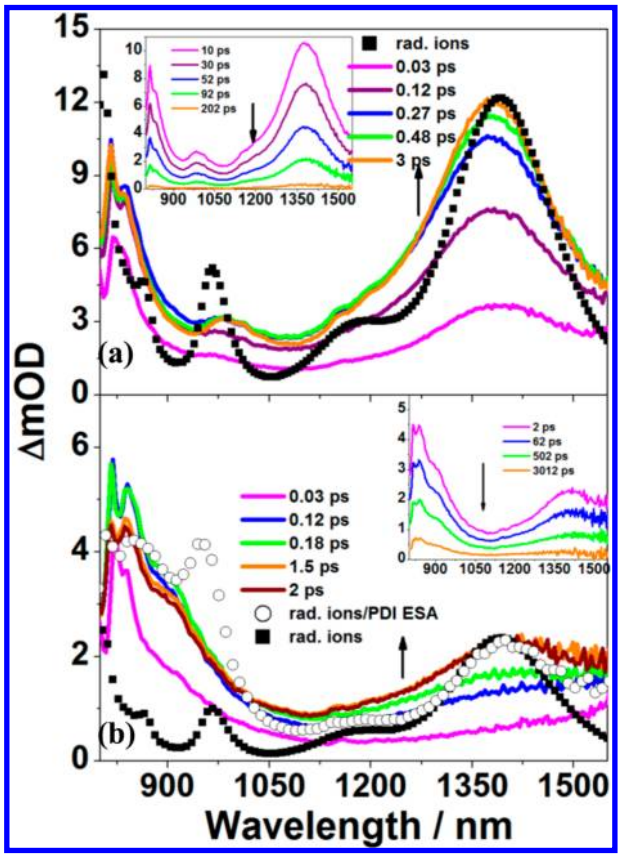


**Figure 8.** TA spectra of (a) 4.4 mM **PDI-5T** in toluene, excited at 650 nm (OD = 0.48). (b) TA spectra of 8 mM **5T** and 4 mM **PDI** co-dissolved in toluene, excited at 650 nm (OD = 0.31). The insets present the long-time dynamics, and the ordinates are in ΔmOD. Black squares in both plots represent the scaled sum of the **5T** and **PDI** RIA spectra. Circles in (b) represent the scaled sum of the radical ions added to the **PDI** ESA.

PDI radical anion absorption at 965 nm appears almost immediately following excitation, and the rise time of the 5T radical cation absorption band at 1380 nm is also IRF-limited. This indicates that CS is faster than that observed in dilute solution, as shown in Figure 9. The recombination rate, in this case, can be described by a single-exponential decay with a lifetime of 52 ps (Figure S6a, inset, Supporting Information). The single-exponential decay of the radical cation observed for concentrated **PDI-5T** suggests that the donor−acceptor distance is relatively constant, as would be expected in the case of CT complex formation and in contrast to the situation for dilute solutions. These results provide evidence of rapid intermolecular CS and CR within the aggregates as the donor and acceptor groups can be constrained to adopt a much narrower distribution of distances than would be possible in nonaggregated molecules in dilute solutions.

To compare the dynamics of CT of the **PDI-5T** triad to the aggregates of **5T** and **PDI**, co-dissolved at high concentrations, we performed TA measurements on these aggregate-containing solutions, with excitation into the CT absorption tail at 650 nm, as shown in Figure 8b. Unlike the case of **PDI-5T**, the TA spectrum of the concentrated co-dissolved solution of **5T** and **PDI** does not match the spectrum of the radical ion pair at any

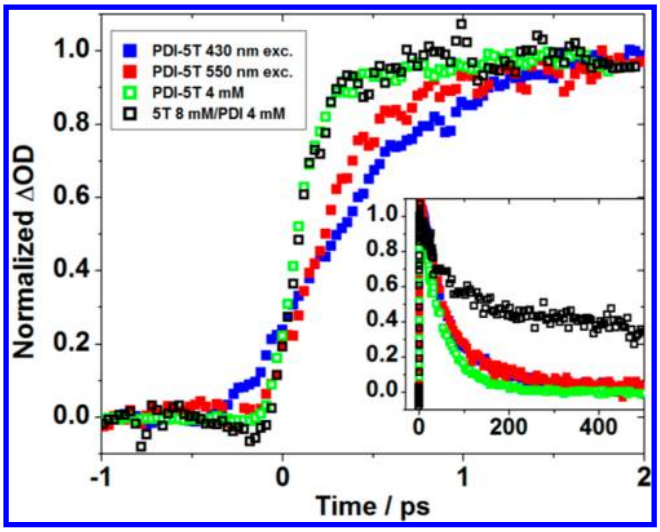


**Figure 9.** Rise times of the radical cation band for dilute solutions of **PDI-5T** in toluene, excited at 430 (5T moiety) and 550 nm (PDI moiety), as well as 4 mM **PDI-5T** and the solution of co-dissolved 8 mM **5T** and 4 mM **PDI**, excited at 650 nm. (Inset) Decay of the radical cation band, and the ordinate is in normalized ΔOD.

delay time. A broad ESA band assigned to the radical cation was observed at 1415 nm, appearing with an IRF-limited rise time (Figure S6b, Supporting Information), indicating rapid CS. The presence of the **5T** radical cation in the co-dissolved solution is further supported by considering the ESA properties of concentrated **PDI** in toluene, which shows no structured absorption band at 1415 nm (see Figure S7a, Supporting Information). The characteristic PDI anion peak at 965 nm is not observed in the concentrated **5T**/**PDI** co-dissolved solution, most likely because it is masked by a strong contribution from ESA of the free/noninteracting **PDI** molecules. Such species would be long-lived compared to those observed in the spectra of concentrated **PDI-5T** because there are fewer donor molecules available locally to quench them.

To address the possibility that the long-lived **PDI** ESA is masking the spectrum of the radical anion, we overlaid a composite plot of the sum of the **PDI** ESA and RIA spectra onto the observed TA, as shown in Figure 8b. The summed spectrum matches the peak of the **5T** radical cation absorption, at 1415 nm, and the short wavelength side of the absorption spectrum at 875−900 nm, but it also contains the distinct radical anion feature at 965 nm that is not apparent in the TA spectra. However, as shown in the TA spectra of the triad excited at 650 nm, Figure 8a, the broadness of the TA spectra relative to the radical ion spectra reduces the apparent contribution from the PDI radical anion to the final spectrum. A sufficiently large contribution from the **PDI** ESA may be enough to completely conceal it, leaving only the shoulder at 900 nm, shown in Figure 8b.

Because the solution consists only of the model compounds, the rates of excited-state quenching and radical ion recombination will depend on the distribution of distances and orientations between the molecules in solution at the time of excitation. Molecules outside of the CT range will exhibit CS and CR that is dependent on the collision rate in the stirred solution. As a result, decay curves are expected to be nonexponential, and we used a biexponential decay function as an approximate fitting function. In the case of direct


dx.doi.org/10.1021/jp409065b | J. Phys. Chem. A 2014, 118, 110−121

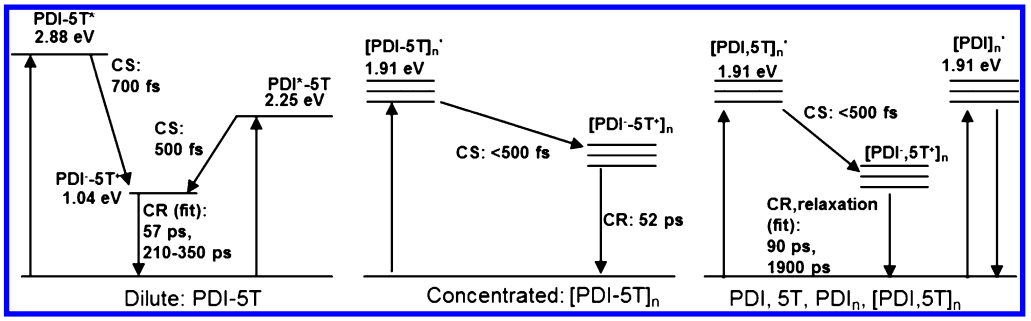


**Figure 10.** Proposed mechanisms for dynamics following excitation of (left) **PDI-5T**, (middle) concentrated **PDI-5T**, and (right) a **PDI/5T** mixture. In the middle and right schemes, species subscripted with an "n" indicate aggregates, and excitation energies in eV correspond to 650 nm.

excitation into the CT absorption tail, the CS rate can be IRF-limited. However, excited **PDI** with no nearby quenchers will exhibit a long lifetime, which explains why the TA from the concentrated mixture solution is still observable after 3 ns. Similarly, the radical ion CR rate can be very long-lived. The decay of the 5T cation absorption can be fitted with a double-exponential function with lifetimes $\tau$ = 90 ps and 1.9 ns, illustrating both the short- and long-distance regimes of CR. On the basis of the time-resolved data, we have constructed Figure 10 to illustrate the dynamics following excitation for each of the systems studied here.

**Nonlinear Optical Pulse Suppression.** Given the ultrafast and efficient CS, along with strong radical ion absorptivities in both **PDI-5T** solutions and concentrated solutions of **PDI** and **5T** model compounds, we investigated the performance of these CT systems as materials for nonlinear optical pulse suppression (defined as $1/T(E_{max})$). The NLA responses of the **PDI-5T** and the model compound solutions are shown in Figure 11. For the individual **5T** and **PDI** solutions, the energy-dependent transmittance curves are indicative of a 2PA-induced ESA (2PA-ESA) absorption response at each of the measurement wavelengths, which is characterized by a high turn-on energy and a subsequent steep reduction of the transmittance. The co-dissolved **5T** and **PDI** solutions, especially at the higher concentration, show a more gradual reduction of transmittance prior to the steep reduction, which is indicative of a 1PA-induced ESA (1PA-ESA) contribution, particularly at the two shorter wavelengths. The 1PA is attributed to the presence of CT complexes of **5T** and **PDI**. At 680 nm, the steep reduction is largely masked by the gradual reduction in transmittance, indicating that the 1PA-ESA is dominating the overall response. On the other hand, the solutions of **PDI-5T** appear to be dominated by the 1PA-RIA response at all three wavelengths, with the turn-on energy reducing somewhat as the wavelength is shortened.

We can quantify the nonlinear response in terms of the optical pulse suppression figure-of-merit (FOM), which is defined as

$$\mathrm{FOM} = \frac{T_{lin}}{T(E_{max})} \tag{1}$$

where $T$ is the transmittance, $T_{lin}$ is the linear transmittance of the sample at the excitation wavelength, and $E_{max}$ is the pulse energy just prior to optical breakdown or nonlinear scattering, which was identified by an abrupt change in slope and much lower S/N at high energies. Further measures of the response include the threshold energy, $E_{Th}$, at which the transmittance is midway between $T_{lin}$ and $T(E_{max})$

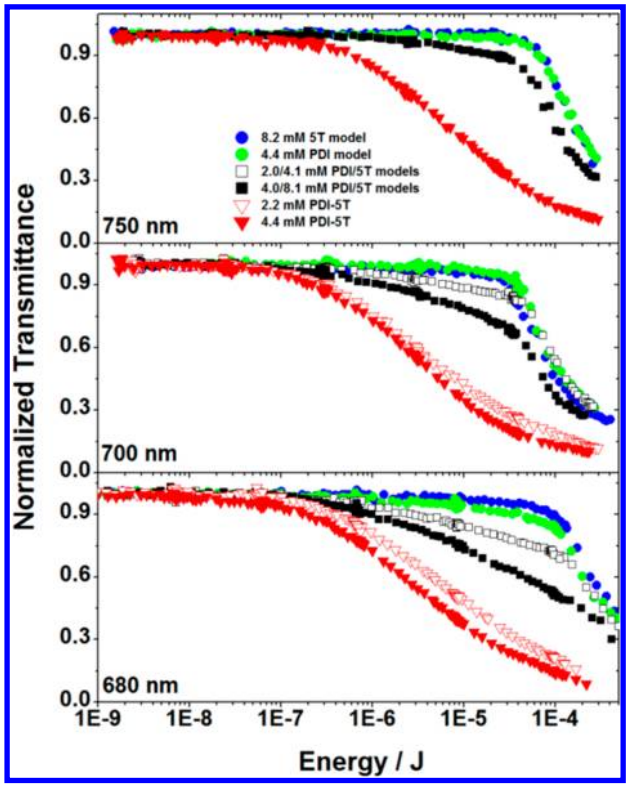


**Figure 11.** Normalized, energy-dependent transmittance curves for **PDI-5T** and model compounds co-dissolved in toluene, using 750, 700, and 680 nm incident light. Excitation was focused in an f/5 geometry into the center of a 2 mm cuvette. The diameter of the beam at the focus, measured in air, was 14 $\mu$m.

$$E_{th} = E\left[\frac{T_{lin} + T(E_{max})}{2}\right] \tag{2}$$

The values of $T_{lin}$, $E_{th}$, and FOM are given in Table 3 and used to compare the response of each solution at the different excitation wavelength.

At high concentration (8 mM for **5T** and 4 mM for PDI), the **5T** and **PDI** solutions show very little 1PA between 680 and 750 nm measurements, suggesting that nonlinear attenuation at the excitation wavelengths is due only to 2PA-ESA. Although **5T** and **PDI** show very different 2PA and ESA band shapes and cross section values, the doubling of the **5T** solution concentration relative to **PDI** results in a similar optical pulse suppression behavior for the two solutions over the wavelengths examined, as shown in Figure 11. Both model compounds show similar suppression values at 680, 700, and


dx.doi.org/10.1021/jp409065b | J. Phys. Chem. A 2014, 118, 110−121

**Table 3. Nonlinear Optical Pulse Suppression Parameters and FOM Values for Solutions of PDI-5T and 5T and PDI Compounds**

| | 680 nm | | | 700 nm | | | 750 nm | | |
|---|---|---|---|---|---|---|---|---|---|
| sample | $T_{lin}$ | $E_{th}$[d] | FOM[e] | $T_{lin}$ | $E_{th}$[d] | FOM[e] | $T_{lin}$ | $E_{th}$[d] | FOM[e] |
| **5T**[a] | 1.0 | 170 | 2.5 | 1.0 | 65 | 3.0 | 1.0 | 120 | 2.6 |
| **PDI**[a] | 0.94 | 170 | 2.6 | 0.95 | 63 | 3.2 | 1.0 | 110 | 2.4 |
| 2:1 **5T/PDI**[a] | 0.80 | 22 | 3.2 | 0.95 | 40 | 3.6 | 0.96 | 75 | 3.2 |
| 2:1 **5T/PDI** dil.[b] | 0.90 | 150 | 3.2 | 0.97 | 70 | 3.3 | | | |
| **PDI-5T**[c] | 0.44 | 3.5 | 14 | 0.48 | 3.4 | 11 | 0.65 | 8.1 | 8.0 |
| **PDI-5T** dil.[c] | 0.65 | 7.0 | 7 | 0.68 | 2.7 | 11 | | | |

[a]**5T** and **PDI** were prepared at 8 and 4 mM in toluene, respectively. 2:1 **5T/PDI** contains both model compounds at concentrations of 8 and 4 mM, respectively. [b]2:1 **PDI/5T** dilute samples contain **5T** and **PDI** compounds at 4 and 2 mM, respectively. [c]**PDI-5T** was prepared at 4 mM concentration, and **PDI-5T** dilute was prepared at 2 mM in toluene. [d]$E_{th}$ is the threshold energy (in $\mu$J), as defined in the text. Uncertainty in $E_{th}$ is 25%. For solutions that exhibited two processes in the energy-dependent NLA curves (e.g., 1PA- and 2PA-induced suppression), the threshold values are effective thresholds calculated with eq 2. [e]FOM is evaluated at the $E_{max}$ prior to damage. The uncertainty in FOM is 25%.

**Table 4. 2PA Cross Sections and Transient Species Molar Absorptivities**

| | 680 nm | | 700 nm | | 750 nm | |
|---|---|---|---|---|---|---|
| sample | 2PA[a] | molar absorptivity[b] | 2PA[a] | molar absorptivity[b] | 2PA[a] | molar absorptivity[b] |
| **5T** | 37 | 4.7 | 46 | 5.1 | 35 | 6.5 |
| **PDI** | 280 | 1.2 | 230 | 1.8 | 15 | 2.0 |
| **5T** cation | | 1.6 | | 2.0 | | 5.8 |
| **PDI** anion | | 2.4 | | 3.7 | | 3.0 |
| total ion | | 3.9 | | 5.6 | | 8.7 |

[a]2PA cross section (in GM; 1 GM = $1 \times 10^{-50}$ cm$^4$ s/photon−molecule) with an uncertainty of ±15%. [b]For **5T** and **PDI**, absorptivity is given in units of $10^4$ M$^{-1}$ cm$^{-1}$ as determined by the singlet depletion method.[38] Absorptivities ($10^4$ M$^{-1}$ cm$^{-1}$) of **5T** cation and **PDI** anion were obtained from spectroelectrochemistry.

750 nm. The FOM of **5T** shows a small increase near 700 nm, which is where its 2PA cross section is largest. The small increase in ESA strength between 700 and 750 nm is insufficient to compensate for the reduction in 2PA cross sections between those two wavelengths; therefore, the overall suppression at 750 nm is still slightly below that at 700 nm. The 2PA cross section determined for **PDI** is somewhat higher at 680 nm than that at 700 nm, and it is rather small at 750 nm, while its ESA is strongest at 750 nm and becomes progressively weaker at 700 and 680 nm. The very weak 1PA at 680 nm by **PDI** results in a slight 1PA-activated component, in addition to a 2PA-activated component in the NLA response, but the overall optical suppression by **PDI** at 680 nm remains low, despite the presence of the weak 1PA component.

A solution containing both 8 mM **5T** and 4 mM **PDI** exhibits stronger linear absorption in the band edge than expected from the sum of the molar absorptivities of the model compounds. As stated above, this is attributed to the formation of intermolecular aggregates, and direct 1PA by excitation into the CT band was shown to generate radical ions in solution. Accordingly, the solution of both model compounds exhibited low-energy thresholds at all wavelengths, which is attributed to 1PA-activated processes due to the aggregate CT absorption.

Despite the enhanced production of radical ions, which show a maximum absorption at 750 nm, the observed FOM values follow the same trend as that with the individual model compounds, with a slightly higher performance at 700 nm, and the suppression values are not much higher than those for the individual model compounds. At 680 nm, the 1PA-activated processes play a more dominant role, likely due to production of radical ions and/or reduction of the intensity at the focus due to the increased CT 1PA, such that the intensity required to activate the 2PA process is not realized before $E_{max}$ is reached. This is supported by the result of dilution of the co-dissolved model compounds by a factor of 2, which reduces the pulse attenuation by 1PA-ESA/-RIA, thereby allowing the 2PA-activated pulse suppression component at 680 nm to turn on at ∼150 $\mu$J. The fact that the overall suppression changed very little from the model compounds and that it followed approximately the same trend suggests that the increased production of radical ions is partially offset by the increased recombination rate of the radical ions in concentrated solutions.

Optical pulse suppression by **PDI-5T** is observed to be dominated by the 1PA-RIA, as expected from the greater number of photogenerated radical ions. In contrast to both the co-dissolved model compound solution and the solutions of the individual model compounds, the suppression observed at 680 nm is similar to that observed at 700 nm, where significantly higher RIA is observed. Two-fold dilution of the **PDI-5T** solution does not significantly reduce the optical suppression of 680 and 700 nm pulses, indicating that the increased 1PA due to intermolecular aggregation is not the only contributor to the optical suppression. We therefore consider the longer lifetime of the CS state in nonaggregated conditions as a possible factor.

Our TA measurements show that in the concentrated solutions, using 650 nm excitation, photogenerated radical ion lifetimes are much shorter than the 6 ns pulses used for optical pulse suppression experiments. For the solution of co-dissolved model compounds, a small population of radical ions was generated, and their lifetimes were short, suggesting that the NLA is dominated by the longer-lived excited states of the nonaggregated species. The optical suppression observed from **PDI-5T**, however, follows the shape of the linear absorption spectrum more closely than the RIA spectrum. A possible explanation is that under these conditions, the generation of a larger number of radical ions via 1PA may be more important


dx.doi.org/10.1021/jp409065b | J. Phys. Chem. A 2014, 118, 110−121

than the actual absorption strength of the radical ions; therefore, the performance scales most strongly with the 1PA strength.

To gain more insight into the optical pulse suppression behavior of the **PDI-5T** triad, nonlinear beam propagation numerical simulations[39] were performed in order to model the nonlinear pulse suppression of **PDI-5T**, **5T**, and **PDI** solutions under high-energy nanosecond excitation at 700 nm. Figure S8 (Supporting Information) displays the results of the fitting as well as experimental results at 700 nm from Figure 11, for comparison purposes. Parameters such as ESA and RIA cross sections, lifetimes, and decay rates were taken from Tables 2−4 in order to perform numerical simulations for **5T**, **PDI**, and **PDI-5T** solutions. To account for the triplet absorption of **5T** at 700 nm, literature values for the triplet ESA cross section and the lifetime of 5T's were adopted.[22,33] As mentioned above, the high linear transmission and the presence of overlapping 2PA and ESA bands of **PDI** and **5T** in the visible−red spectral region suggest that the OL mechanism responsible for the pulse suppression is due to 2PA followed by ESA. This is confirmed in Figure S8a and b (Supporting Information), wherein the optical limiting curves of both dyes at 700 nm are well fitted with the 2PA-ESA model, whereas the 2PA-only simulation shows essentially no pulse suppression. In contrast, 2PA-activated processes are not, however, the dominant nonlinear mechanism for the **PDI-5T** triad. As shown in Figure S8c (Supporting Information), the 2PA-RIA model does not account for the low threshold and the large changes in transmission observed at high energies. The low linear transmission at 700 nm ($T_{lin}$ = 0.41) suggests that the primary excitation and generation of the radical ions in **PDI-5T** is due to 1PA, and accordingly, the 1PA-RIA simulation shows a very good correlation with the experimental data. Not surprisingly, including 2PA as an additional excitation process made very little change in the results of the simulation. Although **PDI-5T** is expected to have a significant 2PA cross section at 700 nm, the high intensity needed for 2PA activation of the RIA is not achieved due in part to the beam attenuation by the 1PA along the beam path in the sample solution.

As **PDI-5T** shows a short radical ion CR time constant (52 ps) relative to the pulse width (∼6 ns), the population of the radical ions is limited by steady-state kinetics and is expected to be relatively low. Nonetheless, the observed optical limiting of the nanosecond pulses is reasonably strong, which can be attributed to the large effective molar absorptivity of radical ions at 700 nm. The numerical simulations indicate an effective RIA molar absorptivity, $\varepsilon_{RIA}$, of ∼1 × $10^5$ $M^{-1}$ $cm^{-1}$, which is somewhat larger (by a factor of ∼2) than the effective extinction coefficient of **PDI-5T** radical ions at 700 nm (Figure 4). This may indicate that the presence of intramolecular and intermolecular aggregates and long exposure times in the nanosecond optical limiting measurements, could lead to a reduction in the overall efficiency of radical ion generation, resulting in an apparent increase in the $\varepsilon_{RIA}$. In any case, the threshold energy and suppression of nanosecond pulses by the **PDI-5T** solutions is consistent with a dominance of the 1PA-RIA process.

Some relevant results from the literature on the optical power limiting properties materials based on 1PA- or 2PA-excited ESA or RIA, including bifluorene-substituted phenanthroline-based Ru(II) coordination complexes, poly(2-methoxy-5-(2-ethylhexyloxy)-(phenylenevinylene)) (MEH-PPV) blends with a $C_{60}$ derivative (PCBM) and dioctylphthlate, poly(2,7-carbazole-*alt*-2,7-fluorene) and poly(3,6-carbazole-*alt*-2,7-fluorene), and a series of 4′-tolylterpyridyl platinum(II) complexes with different arylacetylide ligands are summarized in Table S1 (Supporting Information). Notable high linear transmittances and large optical pulse suppression FOMs for nanosecond pulses have been reported for the MEH-PPV/PCBM blend ($T_{lin}$ = 0.76 and FOM = 21) and the Ru(II) complex labeled LT2/RU ($T_{lin}$ = 0.81 and FOM = ∼7), to which the **PDI-5T** ($T_{lin}$ = 0.44 and FOM = 14 at 4 mM; $T_{lin}$ = 0.65 and FOM = 7 at 2 mM, at 680 nm) compares well.

We can also compare the optical suppression performance of **PDI-5T** to that of the donor−acceptor dyad from our previous work, which consisted of a bis(dialkylaminostyryl)carbazole linked to PDI via a phenylene bridge (dyad 1).[4] Both studies examined 2 mM toluene solutions of the nonlinear absorber under excitation at 700 nm and showed that both materials exhibit similar CR rates following CT band excitation. Dyad 1, excited at 750 nm, shows a transient that decays via a biexponential function, with time constants of 31 and 117 ps; **PDI-5T**, excited at 650 nm, shows a transient that decays with a 52 ps time constant. The molecules possess very different ground-state molar absorptivities; at 700 nm, the absorptivity is 23 $M^{-1}$ $cm^{-1}$ for dyad 1 and 420 $M^{-1}$ $cm^{-1}$ for **PDI-5T**. Despite the ∼18× difference in ground-state absorptivity, the FOM of 5.9, determined for dyad 1, is fairly close to the 6.8 measured for **PDI-5T**. The radical ion absorptivity at 700 nm is significantly higher for dyad 1,[4] but comparison of the suppression at the two wavelengths to the radical ion absorptivity for **PDI-5T** (Tables 3 and 4) suggests that the differences in radical ion absorptivity are not sufficient to overcome differences in ground-state absorption. It is possible that the longer-lived radical ion generated in dyad 1 is leading to more effective integrated NLA relative to **PDI-5T**.

Another factor to consider is the 2PA cross section, which is ∼800 GM for dyad 1 and ∼276 GM for **PDI-5T** (based on the model compound values). Due to the much lower linear absorbance of dyad 1 at 2 mM, the 2PA contribution to the suppression will be much higher than that for **PDI-5T**. Additionally, 2PA can excite nonaggregated molecules, which would otherwise not be excited at 700 nm. As shown in our previous paper, the CR time constant for nonaggregated dyad 1 is 13 ns, which is greater than the excitation pulse duration, and can be expected to have a greater impact on the optical suppression. This shows that, despite the apparent advantages of generating more radical ions by extending the 1PA band via aggregation, there is also a reduced CR time constant that can reduce the steady-state radical ion yield during the pulse.

## ■ CONCLUSIONS

A donor−acceptor−donor triad comprising a central PDI moiety with flanking 5T groups has been synthesized, and its photoinduced CT, CR, and nonlinear optical suppression properties have been characterized. The absorption bands of the radical ions of 5T and PDI overlap spectrally with the 2PA bands of both the donor and acceptor, as well as the 1PA due to aggregates formed at the higher concentrations used. These overlapping bands make a major contribution to the nonlinear optical suppression in the triad. The triad undergoes subpicosecond, photoinduced CS upon excitation of either the 5T or PDI moieties, effectively producing radical ions that facilitate nonlinear suppression of nanosecond laser pulses. This is reflected by the greater FOM of 14 at 680 nm for **PDI-5T** relative to co-dissolved **PDI** and **5T** compounds with a FOM of


dx.doi.org/10.1021/jp409065b | J. Phys. Chem. A 2014, 118, 110−121

3.2. Despite the relatively rapid CR of the photogenerated radical ions, **PDI-5T** shows increased nonlinear optical suppression as a result of the 1PA of the CT complex, even as the radical ion absorptivity decreases as a function of wavelength, in contrast to the behavior of the solutions of co-dissolved **PDI** and **5T** compounds. This suggests that when a high population of radical ions can be generated, strong optical suppression can be achieved but will be more sensitive to the ground-state absorptivity than to the absorption cross section of the transient species.

The impact of aggregation on nonlinear optical suppression for multichromophoric molecules utilizing photoinduced CS provides benefits to the optical suppression in terms of excitation efficiency but also some compromises in terms of the average transient absorber concentration during the laser pulse due to rapid recombination. On the basis of the trends described above, potential routes to improved materials for nonlinear optical pulse suppression would include the use of multichromophoric compounds that have weak broad-band 1PA absorption or large 2PA cross sections for high excitation efficiency that can undergo sequential CT processes to reduce the rate of CR.

## ■ ASSOCIATED CONTENT

### Supporting Information

Synthetic details and chemical characterization; two-photon absorption measurements; fluorescence lifetime measurements; cyclic voltammograms, generation of radical ions, and two-photon absorption spectra; TA kinetics of model compounds; time-resolved fluorescence decays of model compounds; TA kinetics of dilute **PDI-5T**; TA kinetics of concentrated **PDI-5T** and co-dissolved **PDI/5T**; TA and kinetics of concentrated PDI; nonlinear beam propagation simulation of optical pulse suppression; and summary of optical limiting properties for some photoinduced charge-transfer-based materials. This material is available free of charge via the Internet at http://pubs.acs.org.

## ■ AUTHOR INFORMATION


### Corresponding Authors

*E-mail: joe.perry@chemistry.gatech.edu (J.W.P.).
*E-mail: seth.marder@chemistry.gatech.edu (S.R.M.).

### Present Addresses

[†]M.M.S.: RIKEN, Wako 351-0198, Japan.
[‡]C.H.: Polyera Corporation, Suite 140, 8045 Lamon Ave, Skokie, IL, 60077, USA.
[§]N.M.: Los Alamos National Laboratories, Los Alamos, NM 87545, USA.

### Author Contributions

[⊥]The manuscript was written through contributions of all authors. All authors have given approval to the final version of the manuscript. M.M.S. and C.H. contributed equally.


### Notes

The authors declare no competing financial interest.

## ■ ACKNOWLEDGMENTS

This research was supported in part by the MURI Program (50372-CH-MUR) and the DURIP Program (59287-CH-RIP) through the Army Research Office, the STC Program (Center for Materials and Devices for Information Technology Research) of the National Science Foundation (DMR 0120967), the DARPA ZOE Program (Grant No. W31P4Q-09-1-0012), and Solvay S.A.

## ■ REFERENCES


(1) Spangler, C. W. Recent Development in the Design of Organic Materials for Optical Power Limiting. *J. Mater. Chem.* **1999**, *9*, 2013−2020.
(2) Dupuis, B.; Michaut, C.; Jouanin, I.; Delaire, J.; Robin, P.; Feneyrou, P.; Dentan, V. Photoinduced Intramolecular Charge-Transfer Systems Based on Porphyrin−Viologen Dyads for Optical Limiting. *Chem. Phys. Lett.* **1999**, *300*, 169−176.
(3) Belfield, K. D.; Bondar, M. V.; Hernandez, F. E.; Przhonska, O. V. Photophysical Characterization, Two-Photon Absorption and Optical Power Limiting of Two Fluorenylperylene Diimides. *J. Phys. Chem. C* **2008**, *112*, 5618−5622.
(4) Huang, C.; Sartin, M. M.; Siegel, N.; Cozzuol, M.; Zhang, Y.; Hales, J. M.; Barlow, S.; Perry, J. W.; Marder, S. R. Photo-Induced Charge Transfer and Nonlinear Absorption in Dyads Composed of a Two-Photon-Absorbing Donor and a Perylene Diimide Acceptor. *J. Mater. Chem.* **2011**, *21*, 16119−16128.
(5) Huang, C.; Sartin, M. M.; Cozzuol, M.; Siegel, N.; Barlow, S.; Perry, J. W.; Marder, S. R. Photoinduced Electron Transfer and Nonlinear Absorption in Poly(carbazole-*alt*-2,7-fluorene)s Bearing Perylene Diimides as Pendant Acceptors. *J. Phys. Chem. A* **2012**, *116*, 4305−4317.
(6) Hanack, M.; Schneider, T.; Barthel, M.; Shirk, J. S.; Flom, S. R.; Pong, R. G. S. Indium Phthalocyanines and Naphthalocyanines for Optical Limiting. *Coord. Chem. Rev.* **2001**, *219−221*, 235−258.
(7) Balaji, G.; Kale, T. S.; Keerthi, A.; Della Pelle, A. M.; Thayumanavan, S.; Valiyaveettil, S. Low Band Gap Thiophene−Perylene Diimide Systems with Tunable Charge Transport Properties. *Org. Lett.* **2010**, *13*, 18−21.
(8) Huang, J.; Fu, H.; Wu, Y.; Chen, S.; Shen, F.; Zhao, X.; Liu, Y.; Yao, J. Size Effects of Oligothiophene on the Dynamics of Electron Transfer in π-Conjugated Oligothiophene−Perylene Bisimide Dyads. *J. Phys. Chem. C* **2008**, *112*, 2689−2696.
(9) Chen, L. X.; Xiao, S.; Yu, L. Dynamics of Photoinduced Electron Transfer in a Molecular Donor−Acceptor Quartet. *J. Phys. Chem. B* **2006**, *110*, 11730−11738.
(10) Fujitsuka, M.; Harada, K.; Sugimoto, A.; Majima, T. Excitation Energy Dependence of Photoinduced Processes in Pentathiophene−Perylene Bisimide Dyads with a Flexible Linker. *J. Phys. Chem. A* **2008**, *112*, 10193−10199.
(11) Roland, T.; Leonard, J.; Hernandez Ramirez, G.; Mery, S.; Yurchenko, O.; Ludwigs, S.; Haacke, S. Sub-100 fs Charge Transfer in a Novel Donor−Acceptor−Donor Triad Organized in a Smectic Film. *Phys. Chem. Chem. Phys.* **2012**, *14*, 273−279.
(12) Fichou, D.; Horowitz, G.; Garnier, F. Polaron and Bipolaron Formation on Isolated Model Thiophene Oligomers in Solution. *Synth. Met.* **1990**, *39*, 125−131.
(13) An, Z.; Odom, S. A.; Kelley, R. F.; Huang, C.; Zhang, X.; Barlow, S.; Padilha, L. A.; Fu, J.; Webster, S.; Hagan, D. J.; et al. Synthesis and Photophysical Properties of Donor- and Acceptor-Substituted 1,7-Bis(arylalkynyl)perylene-3,4:9,10-bis(dicarboximide)s. *J. Phys. Chem. A* **2009**, *113*, 5585−5593.
(14) Loewe, R. S.; McCullough, R. D. Using Grignard Metathesis to Synthesize Regioregular, Head-to-Tail Coupled Poly(3-substituted)-thiophenes. *Polym. Prepr.* **1999**, *40*, 852−853.
(15) Taranekar, P.; Fulghum, T.; Baba, A.; Patton, D.; Advincula, R. Quantitative Electrochemical and Electrochromic Behavior of Terthiophene and Carbazole Containing Conjugated Polymer Network Film Precursors: EC-QCM and EC-SPR. *Langmuir* **2007**, *23*, 908−917.
(16) Brookins, R. N.; Schanze, K. S.; Reynolds, J. R. Base-Free Suzuki Polymerization for the Synthesis of Polyfluorenes Functionalized with Carboxylic Acids. *Macromolecules* **2007**, *40*, 3524−3526.
(17) Sonogashira, K.; Tohda, Y.; Hagihara, N. A Convenient Synthesis of Acetylenes: Catalytic Substitutions of Acetylenic Hydro-

gen with Bromoalkenes, Iodoarenes and Bromopyridines. *Tetrahedron Lett.* **1975**, *16*, 4467−4470.
(18) Ahrens, M. J.; Tauber, M. J.; Wasielewski, M. R. Bis(*N*-octylamino)perylene-3,4:9,10-bis(dicarboximide)s and Their Radical Cations: Synthesis, Electrochemistry, and Endor Spectroscopy. *J. Org. Chem.* **2006**, *71*, 2107−2112.
(19) Rohr, U.; Kohl, C.; Müllen, K.; Craats, A. V. D.; Warman, J. Liquid Crystalline Coronene Derivatives. *J. Mater. Chem.* **2001**, *11*, 1789−1799.
(20) Keerthi, A. V. Suresh Regioisomers of Perylenediimide: Synthesis, Photophysical, and Electrochemical Properties. *J. Phys. Chem. B* **2012**, *116*, 4603−4614.
(21) Rajasingh, P.; Cohen, R.; Shirman, E.; Shimon, L. J. W.; Rybtchinski, B. Selective Bromination of Perylene Diimides under Mild Conditions. *J. Org. Chem.* **2007**, *72*, 5973−5979.
(22) Becker, R. S.; Seixas de Melo, J.; Maçanita, A. L.; Elisei, F. Comprehensive Evaluation of the Absorption, Photophysical, Energy Transfer, Structural, and Theoretical Properties of $\alpha$-Oligothiophenes with One to Seven Rings. *J. Phys. Chem.* **1996**, *100*, 18683−18695.
(23) Lee, S. K.; Zu, Y.; Herrmann, A.; Geerts, Y.; Müllen, K.; Bard, A. J. Electrochemistry, Spectroscopy and Electrogenerated Chemiluminescence of Perylene, Terrylene, and Quaterrylene Diimides in Aprotic Solution. *J. Am. Chem. Soc.* **1999**, *121*, 3513−3520.
(24) Ford, W. E.; Kamat, P. V. Photochemistry of 3,4,9,10-Perylenetetracarboxylic Dianhydride Dyes. 3. Singlet and Triplet Excited-State Properties of the Bis(2,5-di-*tert*-butylphenyl)imide Derivative. *J. Phys. Chem.* **1987**, *91*, 6373−6380.
(25) Shoaee, S.; Eng, M. P.; An, Z.; Zhang, X.; Barlow, S.; Marder, S. R.; Durrant, J. R. Inter Versus Intra-molecular Photoinduced Charge Separation in Solid Films of Donor−Acceptor Molecules. *Chem. Commun.* **2008**, 4915−4917.
(26) van der Boom, T.; Hayes, R. T.; Zhao, Y.; Bushard, P. J.; Weiss, E. A.; Wasielewski, M. R. Charge Transport in Photofunctional Nanoparticles Self-Assembled from Zinc 5,10,15,20-Tetrakis-(perylenediimide)porphyrin Building Blocks. *J. Am. Chem. Soc.* **2002**, *124*, 9582−9590.
(27) Würthner, F.; Thalacker, C.; Diele, S.; Tschierske, C. Fluorescent J-Type Aggregates and Thermotropic Columnar Mesophases of Perylene Bisimide Dyes. *Chem.—Eur. J.* **2001**, *7*, 2245−2253.
(28) Ford, W. E.; Hiratsuka, H.; Kamat, P. V. Photochemistry of 3,4,9,10-Perylenetetracarboxylic Dianhydride Dyes. 4. Spectroscopic and Redox Properties of Oxidized and Reduced Forms of the Bis(2,5-di-*tert*-butylphenyl)imide Derivative. *J. Phys. Chem.* **1989**, *93*, 6692−6696.
(29) Fichou, D.; Horowitz, G.; Xu, B.; Garnier, F. Stoichiometric Control of the Successive Generation of the Radical Cation and Dication of Extended $\alpha$-Conjugated Oligothiophenes: A Quantitative Model for Doped Polythiophene. *Synth. Met.* **1990**, *39*, 243−259.
(30) DiCésare, N.; Belletête, M.; Marrano, C.; Leclerc, M.; Durocher, G. Conformational Analysis (Ab Initio HF/3-21G*) and Optical Properties of Symmetrically Disubstituted Terthiophenes. *J. Phys. Chem. A* **1998**, *102*, 5142−5149.
(31) Periasamy, N.; Danieli, R.; Ruani, G.; Zamboni, R.; Taliani, C. Location of the Low-Energy $^1A_g$ State in a Polythiophene Oligomer by Two-Photon Absorption Spectroscopy: $\alpha$-Sexithienyl. *Phys. Rev. Lett.* **1992**, *68*, 919−922.
(32) Corrêa, D. S.; Oliveira, S. L.; Misoguti, L.; Zilio, S. C.; Aroca, R. F.; Constantino, C. J. L.; Mendonça, C. R. Investigation of the Two-Photon Absorption Cross-Section in Perylene Tetracarboxylic Derivatives: Nonlinear Spectra and Molecular Structure. *J. Phys. Chem. A* **2006**, *110*, 6433−6438.
(33) Janssen, R. A. J.; Smilowitz, L.; Sariciftci, N. S.; Moses, D. Triplet-State Photoexcitations of Oligothiophene Films and Solutions. *J. Chem. Phys.* **1994**, *101*, 1787−1798.
(34) Chosrovian, H.; Grebner, D.; Rentsch, S.; Naarmann, H. Size-Dependent Transient Behaviour of Thiophene Oligomers Studied by Picosecond Absorption Spectroscopy. *Synth. Met.* **1992**, *52*, 213−225.
(35) Lap, D. V.; Grebner, D.; Rentsch, S.; Naarmann, H. Femtosecond-Spectroscopic Investigations on Bithiophene, Terthiophene and Tetrathiophene in Solution. *Chem. Phys. Lett.* **1993**, *211*, 135−139.
(36) Chosrovian, H.; Rentsch, S.; Grebner, D.; Dahm, D. U.; Birckner, E.; Naarmann, H. Time-Resolved Fluorescence Studies on Thiophene Oligomers in Solution. *Synth. Met.* **1993**, *60*, 23−26.
(37) Hippius, C.; van Stokkum, I. H. M.; Zangrando, E.; Williams, R. M.; Würthner, F. Excited State Interactions in Calix[4]Arene−Perylene Bisimide Dye Conjugates: Global and Target Analysis of Supramolecular Building Blocks. *J. Phys. Chem. C* **2007**, *111*, 13988−13996.
(38) Carmichael, I.; Hug, G. L. Triplet−Triplet Absorption Spectra of Organic Molecules in Condensed Phases. *J. Phys. Chem. Ref. Data* **1986**, *15*, 1−250.
(39) Hales, J. M.; Cozzuol, M.; Screen, T. E. O.; Anderson, H. L.; Perry, J. W. Metalloporphyrin Polymer with Temporally Agile, Broadband Nonlinear Absorption for Optical Limiting in the Near Infrared. *Opt. Express* **2009**, *17*, 18478−18488.